


## BSHAP seismic source characterization models for the Western Balkan region

Jadranka Mihaljević<sup>1</sup>  · Polona Zupančič<sup>2</sup> · Neki Kuka<sup>3</sup> · Nataša Kaluderović<sup>1</sup> · Rexhep Koçi<sup>3</sup> · Snježana Markušić<sup>4</sup> · Radmila Šalić<sup>5</sup> · Edmond Dushi<sup>3</sup> · Enkela Begu<sup>3</sup> · Llambro Duni<sup>3</sup> · Mladen Živčić<sup>2</sup> · Svetlana Kovačević<sup>6</sup> · Ines Ivančić<sup>4</sup> · Vladan Kovačević<sup>6</sup> · Zoran Milutinović<sup>5</sup> · Marjan Vakilinezhad<sup>7</sup> · Tomislav Fiket<sup>4</sup> · Zeynep Gülerce<sup>7</sup>

Received: 31 August 2016 / Accepted: 22 April 2017 / Published online: 29 April 2017  
© Springer Science+Business Media Dordrecht 2017

**Abstract** This manuscript presents the seismic source characterization models that were developed and used for the Western Balkan region in the framework of Harmonization of Seismic Hazard Maps in the Western Balkan Countries Project (BSHAP II) funded by NATO-Science for Peace and Security Program. Relevant knowledge about the geological and seismotectonic structure of Western Balkans and surrounding region was collected and utilized along with the BSHAP focal mechanism database and the BSHAP earthquake catalogue (Markušić et al. in Bull Earthq Eng 14(2):321–343, 2016. doi:[10.1007/s10518-015-9833-z](https://doi.org/10.1007/s10518-015-9833-z)) to delineate seismic source models for different purposes. The super zone model of large zones bounds the regions with similar seismotectonic characteristics and catalogue completeness levels and was used for calculating the regional b-value of the magnitude recurrence relationship. Additionally, two models of smaller zones that represent the epistemic uncertainty in source geometry, maximum magnitude and style-of-faulting, were developed to be employed in the two-stage (circular and elliptical) smoothing procedure. Sets of sensitivity analyses are performed to support final estimates of some models' parameters affecting the smoothed seismicity rate. The seismic source

---

**Electronic supplementary material** The online version of this article (doi:[10.1007/s10518-017-0143-5](https://doi.org/10.1007/s10518-017-0143-5)) contains supplementary material, which is available to authorized users.

---

✉ Jadranka Mihaljević  
jmihaljevic@gmail.com

<sup>1</sup> Institute of Hydrometeorology and Seismology, Podgorica, Montenegro

<sup>2</sup> Slovenian Environment Agency, Ljubljana, Slovenia

<sup>3</sup> Institute of Geosciences, Energy, Water and Environment, Polytechnic University, Tirana, Albania

<sup>4</sup> Faculty of Science, University of Zagreb, Zagreb, Croatia

<sup>5</sup> Institute of Earthquake Engineering and Engineering Seismology (IZIIS), Ss. Cyril and Methodius University, Skopje, Macedonia

<sup>6</sup> Seismological Survey of Serbia, Belgrade, Serbia

<sup>7</sup> Civil Engineering Department, Middle East Technical University, Ankara, Turkey

models and the logic-tree presented here are to be implemented in the probabilistic seismic hazard assessment for the seismic hazard maps of the Western Balkan region.

**Keywords** BSHAP · Seismic source models · Western Balkan region · Magnitude recurrence relationship · Focal mechanism solutions · Maximum magnitude · Spatial smoothing

## 1 Introduction

The *Harmonization of Seismic Hazard Maps for the Western Balkan Countries* Project (BSHAP—SfP #983054) that was founded by NATO Science for Peace (SfP) Program was launched in 2007 and ended in 2011. The follow-up project (BSHAP\_II—SfP #984374, *Improvements in the Harmonized Seismic Hazard Maps for the Western Balkan Countries*) was initiated by the end of 2012. The projects gathered partner institutions from Albania, Bosnia and Hercegovina,<sup>1</sup> Croatia, Macedonia, Montenegro, Serbia, Slovenia (as expert and data providing country) (Fig. 1) and Turkey with the main objective of preparing up-to-date seismic hazard maps for the Western Balkan region.

One of the most stimulating and controversial tasks of BSHAP was the development of the seismic source characterization (SSC) models that are consistent with the seismotectonic and geological characteristics of the area. The key input of the SSC models is the uniform and updated BSHAP earthquake catalogue (described in details by Markušić et al. 2016) which was harmonized from the national catalogues of data providers in the BSHAP area and was enriched with data from global catalogues and catalogues of neighboring countries, especially for large magnitude events. Therefore, the characteristics and the completeness levels of the BSHAP earthquake catalogue show a large temporal and spatial variability, which has a strong effect on the b-value and maximum magnitude estimates as the SSC model's parameters. BSHAP participants put together a profound analysis of the geological structure, active tectonics, and geodynamics of the region to support the earthquake catalogue in delineating the zones with similar seismotectonic characteristics. Information, which is documented in this paper, is the outcome of the BSHAP\_II project and is employed in developing alternative *seismic source models (SSMs)*. A standalone section of this manuscript is devoted to the BSHAP fault plane solutions database, which was prepared with the joint effort of five participating countries including Albania, Croatia, Macedonia, Montenegro, and Serbia and directly implemented in SSC model development.

Similar to the SHARE project (Woessner et al. 2015), we developed a *super zone model (SZM)* of large zones that were delineated based on the seismotectonic characteristics. For each super zone, b-value was calculated using the maximum likelihood estimation (MLE) that considers unequal completeness intervals for different magnitude ranges (Weichert 1980) and the MLE procedure developed by Kijko and Sellevoll (1992, KS-92). Other parameters of the SSC model ( $m_{\max}$ , dominant style of faulting and fault directions) were estimated for smaller areas, delineated within two *alternative zonation models* (seismic source model 1—SSM1 and seismic source model 2—SSM2). SSM1 and SSM2 that represent the local tectonic features provide input data for the two-stage (circular and elliptical) smoothing procedure. Epistemic uncertainty of the b-value, choice of SSM,

<sup>1</sup> Bosnia and Hercegovina did not take part in BSHAP II partnership.

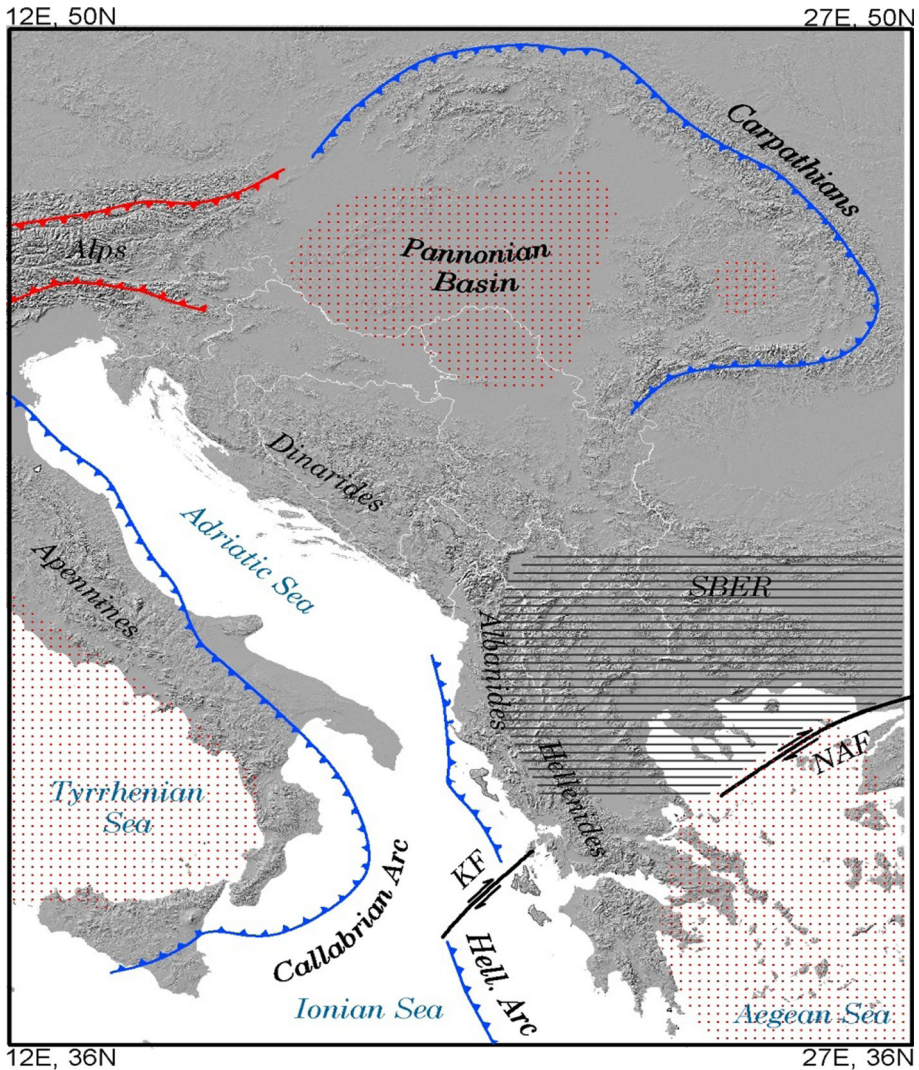


**Fig. 1** Simplified tectonic map (according to Dumurdzanov et al. 2005) of BSHAP region and surroundings showing Southern Balkan Extensional Region (SBER; horizontal lines) in relation to selected tectonic features. Retreating subduction zones (blue) and related areas of backarc extension (dotted pattern) and advancing subduction zones (red) are highlighted. KF—Kefalonia fault zone; NAF—North Anatolian fault zone. Borders of BSHAP participating countries are highlighted with white lines

maximum magnitude ( $m_{\max}$ ) and type of smoothing is included in the logic tree scheme. Sensitivity analyses were conducted to understand the effect some models' parameters have on smoothed seismicity rate and to support modeler's decisions. Both the super zone model and the alternative zonation models are thoroughly described in the forthcoming sections. The BSHAP SSC model, along with the ground motion prediction models chosen by Šalic et al. (2016), is directly utilized in the hazard calculations to derive the seismic hazard maps for the Western Balkan region.

## 2 Geological structure, active tectonics and geodynamics of the Western Balkan region

The geological structure of Western Balkans is strongly affected by the collision between Adria microplate and the south-western Eurasia margin. The most recent geodynamic scheme suggests that Eurasia subducts under the Adria in the whole Alpine region, together with a less pronounced under-thrusting of the Adria beneath the Eurasia at the north-eastern collisional boundary. Along the eastern coast of Adriatic Sea and eastern coast of Ionian Sea, the collision between these two tectonic plates has led to the build-up of Dinaro-Albanian-Hellenic folded structure, which passes through the Aegean Sea to the Turkish Taurids (Fig. 1). On the south, Hellenides are confined by the Hellenic Arc, which has the geological and geophysical features resembling those of the island arcs (Mercier et al. 1979), in contrast with the Adriatic collision with Dinarides and Hellenides on the north. The Hellenic Arc subduction dips from the Hellenic trench towards north-east for approximately 180 km. The transition from the zone of the Hellenic Arc subduction zone to the Adriatic collision (zone of continental subduction) is along the Ionian Islands (Sorel 1976), and accompanied by a transform Kefalonia fault zone (KF in Fig. 1). By taking into consideration the general tectonic features derived from geological and geophysical data, the orientation of 30° NNE was specified for this dextral strike-slip fault with a thrust component, which lies along the western edge of the Kefalonia—Lefkas Islands (Cushing 1985; Sorel 1989; Scordilis et al. 1985).

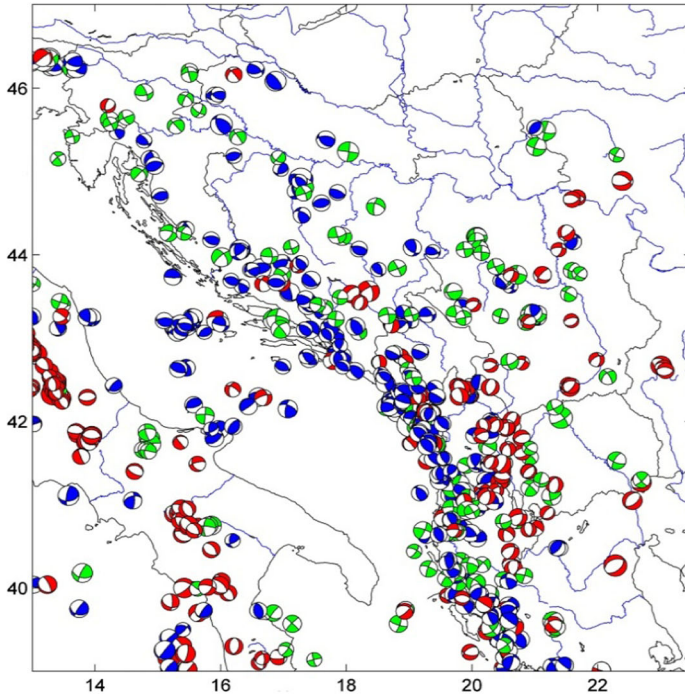
Hellenides on the Greek territory are characterized by a complex tectonic structure. Strike-slip faults, which are documented by the focal mechanisms of earthquakes, can be found on the northern Aegean. Strike-slip faults are noticed also in Marmara Sea, extending in the north Aegean basin as well as in the central Ionian Sea up to north-western Peloponnese. On the other hand, the whole sector from the southern Albania up to northern Peloponnese undergoes a compressive tectonic regime with thrust faults trending mainly in SSE-NNW direction. This regime is supported by the focal mechanisms of some earthquakes located in the south of Albania and along the Ionian coast in Greece.

The interaction between the Dinaro-Albanian-Hellenic range and the tectonic units on the east such as Pannonian basin and Serbian-Macedonian massif played an important role on the formation of geological structure of Western Balkans. The Dinarides are a thrust and fold belt zone of elevated and deformed sediments that stretches along the NW–SE direction from the Southern Alps in the north to the Albanides in the south-east. The passage from Dinarides to Albanides is through the structure of Shkodra-Peja transversal fault (Frashëri et al. 2009). To the north-east, Dinarides are bounded by the Pannonian basin with a wide transition zone in between (Šumanovac et al. 2009; Brückl et al. 2010). The fold-thrust belt of the Dinarides in its north-western and central parts is subdivided into two tectonic domains of External and Internal Dinarides, bounded by the south-eastern Alps and Tisia to the north and north-east, respectively (Tomljenović et al. 2008). The External Dinarides encompass the SW-verging thrust belt formed along the Eastern Adria margin and the NE dipping thrusts of the Central Adriatic. The recent studies (Kastelic and Carafa 2012) on fault slip rates show that the most active portion is the south-eastern part of the External Dinarides (offshore Montenegro and Albania), where the highest average slip rate of 2 mm/year was estimated. The slip rates diminish to the north-west and are lower than 0.15 mm/year for the faults of north-western part of External Dinarides in Slovenia. In this part of the belt, the main deformational phase (known as a ‘Dinaridic phase’) resulted in a quite distinctive NW trend and SW-vergence of km-scale

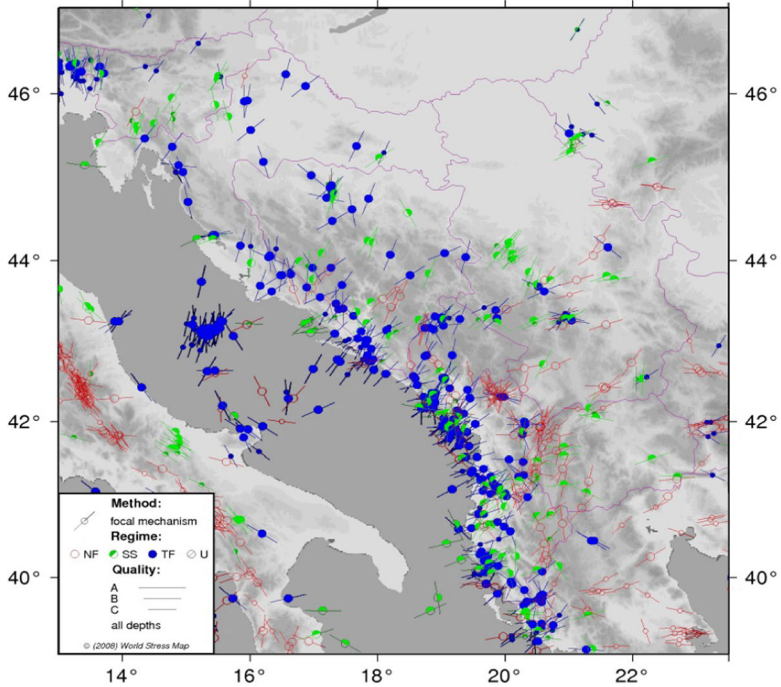
compressional and imbricated structures (Tari-Kovačić and Mrinjek 1994; Blašković 1998). The Internal Dinarides of central and northern Bosnia and Herzegovina and northern Croatia are comprised of the Bosnian flysch zone; the zone composed of nonto low-grade metamorphic units derived from a distal Adriatic Plate margin involved in the Late Jurassic ophiolite obduction.

The Pannonian basin is one of the classical back-arc basins, whereas the Carpathian belt has many characteristics of a classical foreland and fold-and-thrust belt (Cloetingh et al. 2002). The state of present-day stress in the Pannonian–Carpathian system, particularly in its western and southern part is governed by complex interaction of plate boundary and intra-plate forces. Neotectonic structures in the Pannonian region are largely controlled by the reactivation of pre-existing shear zones. Accordingly, reverse faulting in the basement leads to folding of the overlying strata in the west. Towards the east, the style of deformation becomes strike–slip faulting with either transpressional (local shortening) or transtensional (local extension) component (Bada et al. 2007). The Serbian-Macedonian massif and Vardar area are situated in between Balkan Mountains on the east and Dinaro-Albanides belt on the west. The Serbian-Macedonian massif has been considered as an autochthonous central block that has played a main role in the interaction with surrounding geological structures. The recent observations in Eastern Serbia indicate that the local stress field has a significant effect on the recent tectonics of this area: transpressional tectonics is likely influenced by east situated rigid Moesian Promontory, while transtensional tectonic regime marks the onset of the influence of the Pannonian Basin extension (Mladenović et al. 2014). The southern Balkan region is part of the more regional Aegean extensional realm that we refer to as the Southern Balkan Extensional Regime. In Macedonia, late Cenozoic E–W extension shows a progressive migration toward the west where the roll-back of the northern Hellenic trench occurred from Paleogene to recent time (Burchfiel et al. 2006). There are three areas of different tectonism: E-NE shortening along the Adriatic coast, then E-NE to E-W extension ranging from eastern Albania to western Macedonia, and finally N-S extension in eastern Macedonia and Bulgaria (Dumurdzanov et al. 2005).

Albanides are built up by different rock formations varying extensively in age, dated from Paleozoic to Quaternary period. During the pre-neotectonic Alpine evolution, tectonic nappes with considerable amplitude were developed in the inner part of Albanides, while in the outer zone thrust and back-thrust structures can be observed. The convergence of the geological structures in Albanides is oriented towards west and southwest, from the inner part toward the outer one, with the displacement of masses towards southwest (Aliaj 1998; Koçi et al. 2013). The outer areas are still under the influence of a compressive regime (Aliaj 1998; Jouanne et al. 2012). Therefore, they have been dissected by thrust, less present back thrusts, and in some cases strike-slip, active faults. On the other hand, normal faults exist in some specific graben sectors (as Skadar Lake in the north and Butrinti Lake in the south). In the outer area of Albanides, the system of active faults is almost linearly extended, trending in SE-NW direction. In the inner part of the Albanides, an extensional tectonic regime predominates, as confirmed by geodynamic data (Jouanne et al. 2012; Koçi 2014), which has contributed to the N-S oriented normal faults and rarely observed over-thrusts, dissecting and cutting through the area.



(a)



(b)

◀ **Fig. 2** BSHAP FPS database, insert for the geographical area 13–23.5E, 39–47N. *Color of symbols* marks the FPS for different mechanisms: the *blue, red* and *green* symbols stand for the reverse, normal and strike-slip events, respectively. **a** Integrated presentation of fault-plane solutions—lower hemisphere equal-area projections. **b** Tectonic stress regime obtained from BSHAP FPS database is plotted using The World Stress Map by Heidbach et al. (2008). Stress regimes are denoted by: *NF* normal, *SS* strike slip, *TF* thrust and *U* for unknown type of regime

### 3 BSHAP fault plane solutions database

The fault plane solutions (FPS) database that was collected or analyzed by the BSHAP project partners is used in the preparation of SSC models in addition to the general geodynamic characteristics of the region. The FPS database developed in the course of this project includes 714 FPS for  $M \geq 4.0$  earthquakes that occurred between the years of 1909 and 2015 within the area bounded by 38–48N and 12–24.5E. The insert of the database covering BSHAP countries and surrounding area is shown in Fig. 2. Approximately half of included FPS data were collected from global resources such as: The Mediterranean Network (MedNet/The Italian CMT dataset, 303 events), database of L’Istituto Nazionale di Geofisica e Vulcanologia (INGV, 19 events), Harvard Centroid Moment Tensor Catalogue (Harvard CMT, 18 events), database of the United States Geological Survey National Earthquake Information Centre (USGS/NEIC, 12 events), National Observatory of Athens (NOA, 11 events), Zurich Moment Tensors Database (ZUR\_RMT, 8 events), The International Seismological Centre (ISC, 4 events), The GFZ German Research Centre for Geosciences (GEOFON Moment Tensor Solutions, 2 events), the Geology Department at the University of Bristol (Bristol CMT, 2 events), The database of Earthquake Mechanisms for European Area (EMMA, Vannucci and Gasperini 2003, 1 event), McKenzie (1972) (1 event) and Cejkovsk et al. (2008) (1 event). Remaining 332 FPS were analyzed by the project participants or gathered from data held by partner institutes (An updated Croatian FPS Database first described by Herak et al. (1995)—current version of which is presented in Herak et al. (2016), the updated Montenegrin FPS database (Kaluderovic 2015), and the FPS databases of Seismological Survey of Serbia and Institute of Geosciences, Energy, Water and Environment, Albania).

The method of first motion polarities was implemented in the analysis of majority of FPS. In the case that several agencies provided the FPS for the same earthquake, priority was given to the agency on whose territory the earthquake had occurred. Exception to this rule was made in cases when the data holder has attributed a better quality mark to some other agency’s FPS. Once collected and analyzed, FPS data is integrated using the software developed by Prof. M. Herak of the Faculty of Science, University of Zagreb.

Figure 2a shows a portion of the BSHAP FPS database with the focus on BSHAP borders. Different color of beach-ball symbols marks the FPS for different mechanisms: blue, red, and green symbols stand for the reverse, normal, and strike-slip events, respectively. Direction of regional maximal horizontal stress is considered as a good indicator of the dominant tectonic regime in a certain area. The general pattern of the FPS indicates that the majority of the earthquakes observed along the coastlines of Croatia, Montenegro and Albania have reverse mechanism, correlated to the thrusting in the most part of the External Dinarides and Albanides. Tectonic compressions are directed in SW–NE direction in the southern and eastern parts and in S–N direction in the northern and western parts of the coastline. Moving away from the coast towards inland, the faults are active as strike-slip to oblique strike-slip or even as reverse faults. This distribution reflects the counter-clockwise motions of Adria and its compression against the Dinarides. In the

Albanides, the boundary between normal faulting to east and thrust faulting to west runs through central Albania. The extension is observed in eastern Albania and Macedonia (Fig. 2b).

## 4 Seismic source characterization models

Information provided in the previous sections clearly demonstrates that the BSHAP area and surrounding region contain quite diverse tectonic regimes. The BSHAP countries mostly lie in the Adria-Eurasia collision zone, where there are great differences in seismicity rate, present-day stress direction, strain rate, and consequently in fault slip rate among neighboring regions. It is well known that hazard results are sensitive to the seismic sources comprised within and outside the area of calculation, so the broader surroundings of the BSHAP region itself have to be included in the SSC model. Therefore, a larger area bordered by 12–24.5E and 38–48N has been considered in SSC modelling, as well as for the BSHAP catalogue compilation (Markušić et al. 2016).

### 4.1 The super zone model

Current practice of seismic source zonation is either guided by tectonic information where polygons are located around major tectonic structures (e.g. SHARE zonation for Turkey, Greece and Italy), or depends on the pattern of seismicity, where polygons are used to separate the areas with spatially and temporally homogenous seismicity (e.g. other areal source zones of SHARE). The former approach could not be implemented in BSHAP since crucial information related to the fault activity, segmentation models, rupture process documentation, and seismic moment accumulation for the BSHAP region is either missing or heterogeneous. Therefore, the pattern of seismicity that is supplemented by the unified and updated BSHAP earthquake catalogue is the most essential input of the BSHAP SSC model. Even if the BSHAP earthquake catalogue is one of the most complete catalogues that covers the Western Balkan region, it still strongly depends on the global catalogues for the surrounding areas and the completeness levels of the catalogue show a large temporal and spatial variability.

In the areal source zone approach, the premise of uniform seismicity within source zone requires small enough zone areas. That requirement induces undue fluctuations in the recurrence model parameters (b-value, mean annual rate of earthquake occurrence, etc.), particularly in the zones of low seismicity. The large variability of the seismicity parameters in regional zonation is often simply statistical variations due to the small sample sizes. The concept of large areas, a.k.a. the *super zones*, that represents the general pattern of prevalent tectonic regime, catalogue completeness, b-value, maximum magnitude, focal depth distribution and style of faulting was introduced in the SHARE project (Woessner et al. 2015).

We adopted a similar approach and created a *super zone model* (SZM) that includes 7 larger areas and 2 smaller zones, as shown in Fig. 3. The delineation of the super zones was based on the alternative zonation models (described later). Super zones were built by merging the seismic source zones considering the tectonic constraints, dominating stress regime, and catalogue completeness behavior. The super-zone ALP1 includes the area north of the Periadriatic line and the Transdanubian range (Poljak 2000a). The PAN2 super-zone covers the Pannonian basin and the Carpathyan belt. The super-zone DIN3



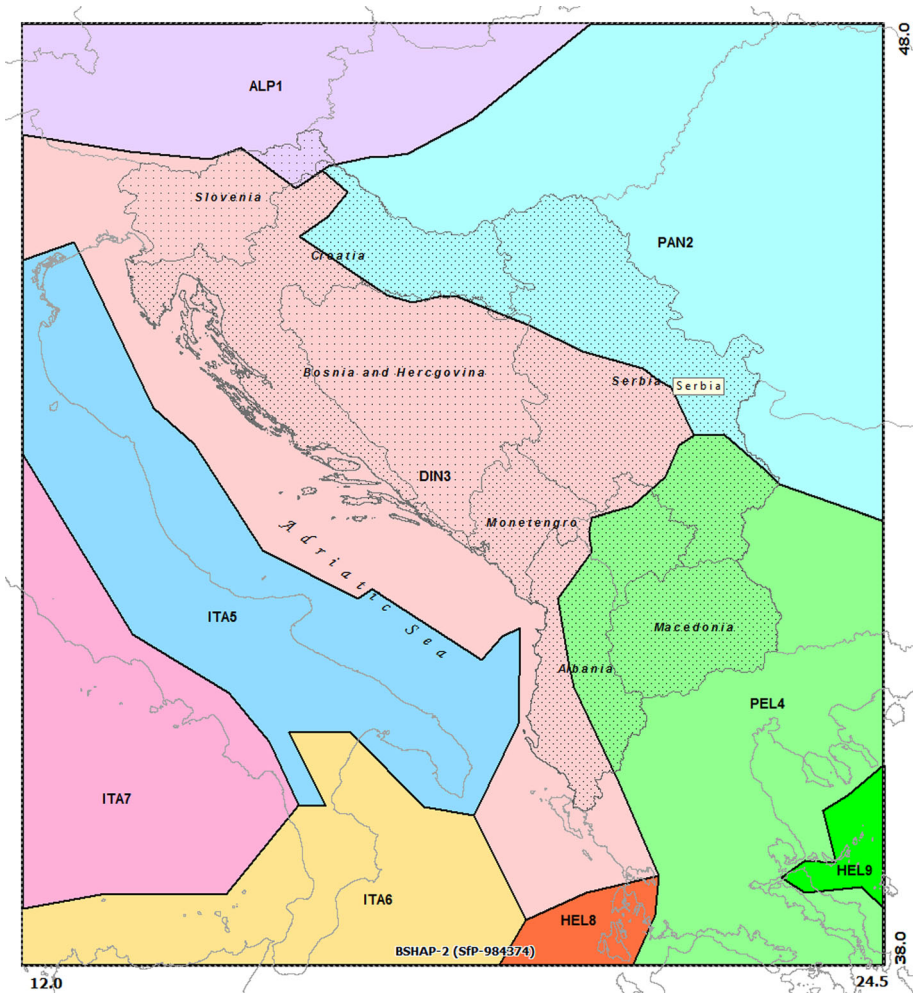


**Fig. 3** Super zone model (SZM) is defined for influence area covering 12–24.5E and 38–48N. Western Balkan (BSHAP\_II partners’) countries Albania, Croatia, Macedonia, Montenegro and Serbia are shown as well as Slovenia (as expert and data providing country). In the first BSHAP project Bosnia and Herzegovina took part as a partner country

includes the area of Southern Alps, External and Internal Dinarides and Albanides. The super-zone PEL4 covers the Southern Balkan extension regime zone. The super-zones ITA5 to ITA7 are delineated based on the SHARE project (Woessner et al. 2015): ITA5 covers the territory of very active structures of central and eastern Apennines and part of the western Adriatic, ITA6 is dominated by subduction in the Calabrian Arc, and ITA7 covers the seismically not very active part of the Tyrrhenian Sea. The delineation and tectonics of smaller zones within Greece (zones HEL8-Cephalonia and HEL9-North Aegean) are adopted from the model proposed by Vamvakaris et al. (2013). HEL8 includes the northern central Ionian Islands (Kefalonia and Lefkada) and exhibits the highest seismicity levels in the whole study area. Large dextral NE–SW to NNE–SSW strike-slip faults are found in this area, interrupting the reverse faulting pattern transition from the

southern Adriatic and NW Greek coast to the South Ionian Sea and the western section of the Hellenic arc (Vamvakaris et al. 2013). On the other hand, significant dextral strike-slip faulting observed in the northern Aegean area (HEL9) is related to the horizontal displacement of the Anatolia microplate parallel to the Anatolian fault, towards the west (Vamvakaris et al. 2013).

Due to imposed rectangular models 'geometry, some of the super zones are not complete in space, have large portions of sea (where historical seismicity suffers documentation), or are naturally of lower seismicity and thus, cause problem in b-value determination. On the contrary, adopted smaller zones—HEL8 and HEL9, are characterized by a very dense seismic activity and large sample sizes, which enable a reliable estimation of the relevant b-values. It is noteworthy that central and substantial part of the BSHAP area is located in the super zone named DIN3. The BSHAP catalogue is the most reliable source to estimate the earthquake recurrence parameters for DIN3 zone. The earthquake data included from available national or global catalogues for neighboring non-BSHAP countries e.g. Italy, Austria, Hungary, Greece, strongly affected recurrence in other SZM zones (Markušić et al. 2016).

Completeness time intervals of the BSHAP earthquake catalogue in each super zone are estimated for different magnitude of completeness ( $M_c$ ) i.e. for the smallest value of magnitude at which the catalogue is thought to have included all seismic events.  $M_c$  was estimated based on its departure from the linear frequency-magnitude relation (Wiemer and Wyss 2000; Mignan and Woessner 2010) using the methodology defined in Markušić et al. (2016) and the results are tabulated in Table 1. In general, the BSHAP catalogue includes the earthquakes with  $M_w \geq 3.0$ , but not all the events with  $M_w \geq 3.0$  are included in each super zone, especially for the regions outside the territory of BSHAP participating countries. Ignoring the spatial variability of  $M_c$  can lead to erroneous results of the seismicity parameters, especially the b-value. Analyzing changes in seismic rates also requires an accurate determination of the  $M_c$ . Considering that, the minimum magnitude ( $m_0$  in Fig. 4) is set to 4.0 for all super zones.

On the other hand, the upper magnitude had to be filled in by inference due to long recurrence interval of the large magnitude earthquakes. Therefore, maximum magnitude accepted in the MFD model ( $m_{\max}$  in Fig. 4) is set by adding 0.25 magnitude unit to the

**Table 1** Completeness of the BSHAP earthquake sub-catalogues over magnitude classes

	Completeness ( $M_c$ )/complete from year							
	[4.0, 4.5)	[4.5, 5.0)	[5.0, 5.5)	[5.5, 6.0)	[6.0, 6.5)	[6.5, 7.0)	[7.0, 7.5)	[7.5, 8.0)
ALP1	1958	1935	1920	1900	1640	1300	1300	1300
PAN2	1965	1915	1880	1835	1565	1300	1300	1300
DIN3	1965	1955	1905	1830	1600	1400	1250	1100
PEL4	1932	1908	1870	1820	1760	1400	1400	1400
ITA5	1960	1930	1850	1750	1650	1360	1360	1360
ITA6	1945	1910	1895	1840	1780	1650	1650	1650
ITA7	1930	1910	1850	1740	1640	1300	1300	1300
HEL8	1950	1902	1870	1825	1770	1625	1625	1625
HEL9	1975	1960	1940	1908	1590	1300	1300	1300

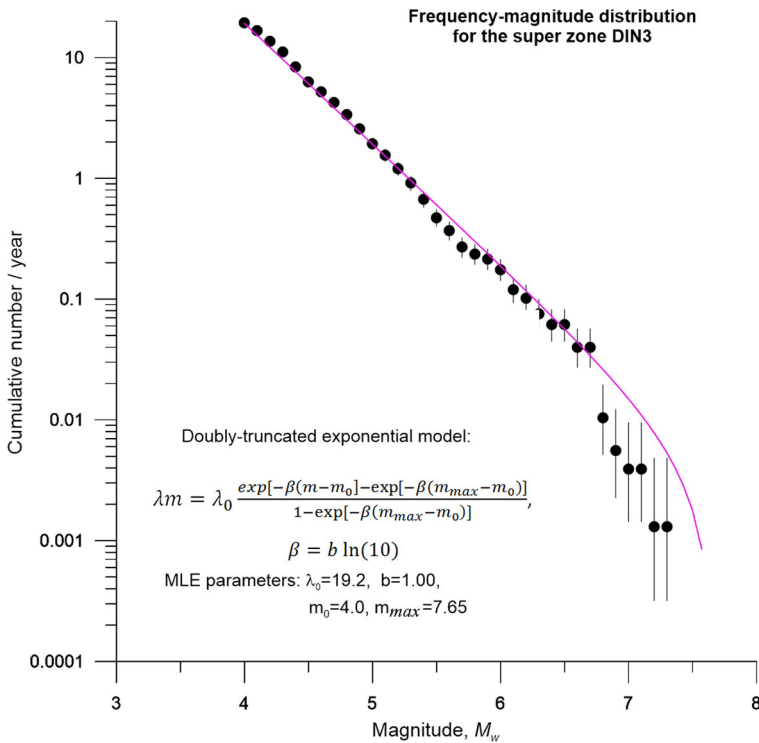


**Fig. 4** Modeling of the magnitude-frequency distribution (case of the super zone DIN3)

largest observed magnitude in each super zone, and the assigned value is evaluated by considering the earthquake catalogue and existing knowledge of seismogenic zones (as in Table 2 of this paper and Electronic supplement—Table 2, as well).

**Table 2** The recurrence parameters for the super zones

Super zone	MLE ( $M_w \geq 4.0$ )				KS-92 ( $M_w \geq 4.0$ , $R = 30$ km)			SHARE (as model)	
	#Events	b-value	$m_{\max}$ obs	$m_{\max}$	#Events	b-value	$m_{\max}$	b-value	$m_{\max}$
ALP1	11	0.79	6.54	6.75	38	–	–	1.00	6.75
PAN2	56	0.83	6.50	6.75	197	1.02	6.20	1.00	6.75
DIN3	1505	1.00	7.37	7.65	1935	1.09	7.98	1.00	7.65
PEL4	1659	1.16	7.51	7.75	1751	1.02	7.59	0.89	7.75
ITA5	195	0.68	6.95	7.15	143	1.03	6.84	1.00	7.15
ITA6	111	0.77	6.95	7.15	250	1.00	7.17	1.00	7.45
ITA7	35	0.68	6.54	6.75	515	0.98	7.23	1.00	7.45
HEL8	386	1.10	7.40	7.65	185	1.09	7.55	0.80	7.65
HEL9	186	1.34	7.16	7.45	391	1.10	7.64	1.00	7.45

Initial estimates of the  $b$ -values and  $\lambda_0$  (mean annual rate of the earthquakes with magnitude greater or equal to  $m_0$ ) of the double truncated exponential magnitude recurrence model for the super zones are obtained using the maximum likelihood (MLE) method proposed by Weichert (1980) that considers the unequal completeness intervals for different magnitude ranges. Figure 4 presents the MLE fit for the super zone DIN3, as well as the relevant BSHAP earthquake data points and the related uncertainty (error bars showing the 95% confidence bounds). The MLE estimates using Weichert (1980) procedure for the other super zones are provided in Electronic supplement (Fig. 1). The MLE estimates of  $b$ -values described above are based only on the complete parts of the BSHAP earthquake catalog over magnitude classes. Thus, the number of events and the time span of the BSHAP catalog is significantly reduced in MLE estimation process.

To make use of all available data (complete and the extreme parts of the BSHAP catalog), we also applied the maximum likelihood procedure developed by Kijko and Sellevoll (1992), briefly referred as KS-92, to estimate the  $b$ -value and the  $m_{max}$  for the super zones. The KS-92 procedure is capable of accounting for the uncertainties of occurrence times of the prehistoric earthquakes. Uncertainty in earthquake magnitude is taken into account, by assuming that the observed magnitude is the true magnitude subjected to a random error that follows a Gaussian distribution having zero mean and a known standard deviation.

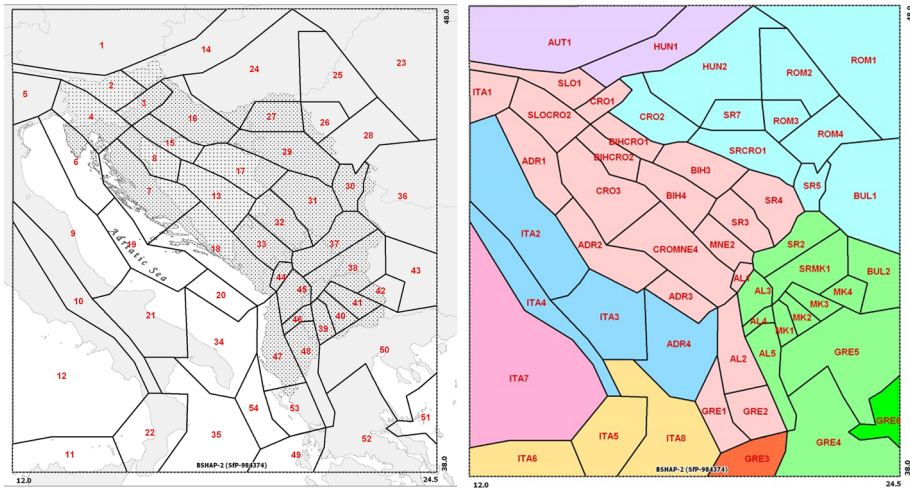
Again, the completeness intervals given in Table 1 are utilized in KS-92 procedure. Adopted calculation grid is  $0.1^\circ \times 0.1^\circ$  for the KS-92 procedure in longitude and latitude with the radius of smoothing of  $R = 30$  km. For each super zone, the KS-92 parameters are calculated from the grid cells.  $b$ -value is the weighted average of the  $b$ -values in the grid cells located in the relevant zone, and  $m_{max}$  is the maximum of the  $m_{max}$  values of the grid cells located in that particular zone. The magnitude recurrence parameters ( $b$ ,  $m_{max}$ ) estimated by the KS-92 procedure are compared to the relevant values from the MLE approach defined by Weichert (1980), as well as the relevant estimates obtained in the framework of the SHARE project for the areal source MLE model (AS Model, Basili et al. 2013) (Table 2).

Table 2 shows that the number of the events accounted for  $b$ -value estimation using the standard MLE for the super zones ALP1, PAN2, ITA5, ITA6, ITA7 and HEL9 is too small. Therefore, the relevant obtained estimates cannot be considered reliable. The  $b$ -value estimates obtained for the super zones characterized by large datasets (DIN3, PEL4, HEL8) are compatible with the relevant KS-92 estimates. On the other hand, KS-92 estimate of  $b$ -value is also very stable in all super zones, varying from 0.98 to 1.10. For altered radius of smoothing ( $R = 40$  km), the KS-92 estimates of  $b$ -value are slightly higher, but show significant stability of results, as well (Table 2 of the Electronic supplement).

We decided to take into account both of the results from the Table 2—the standard MLE and the KS-92 ( $R = 30$  km) estimate of  $b$ -value, using the respective average  $b$ -value for each super zone. These average  $b$ -value estimates vary from 0.79 (ALP1) to 1.2 (HEL9). An alternative option in the relevant logic tree branch is using of  $b = 1.0$  in all super zones. That is consistent with the  $b$ -values estimates recommended in the SHARE project for the super zones comprised in the BSHAP region (Table 2; Fig. 5).

#### 4.2 Alternative zonation models—SSM1 and SSM2

While the super zone model has been implemented with the purpose of estimating statistically-stable  $b$ -values, two alternative seismic source models (SSM1 and SSM2) were



**Fig. 5** Geographical partition of SSM1’s zones and their position versus super zone model. BSHAP countries are indicated by dotted pattern

constructed for providing geographical constraints on the calculation of the fault type, strike angle and  $m_{max}$ , and to handle the epistemic uncertainties related to source geometry. SSM1 and SSM2 were defined by dividing the whole region into areas with homogenous seismotectonic characteristics as shown in Figs. 5 and 6. The experts from partner countries proposed, discussed, and harmonized the zonation for their territories and the neighboring areas to establish these models. SSM1 and SSM2 were developed, considering a detailed analysis of tectonic settings, known active faults, activity rates, observed magnitudes, and foci depths. Figures 5a and 6a show that the zones of SSM1 are slightly larger than the zones of SSM2 (SSM1 consists of 54 zones, while SSM2 encompass 65

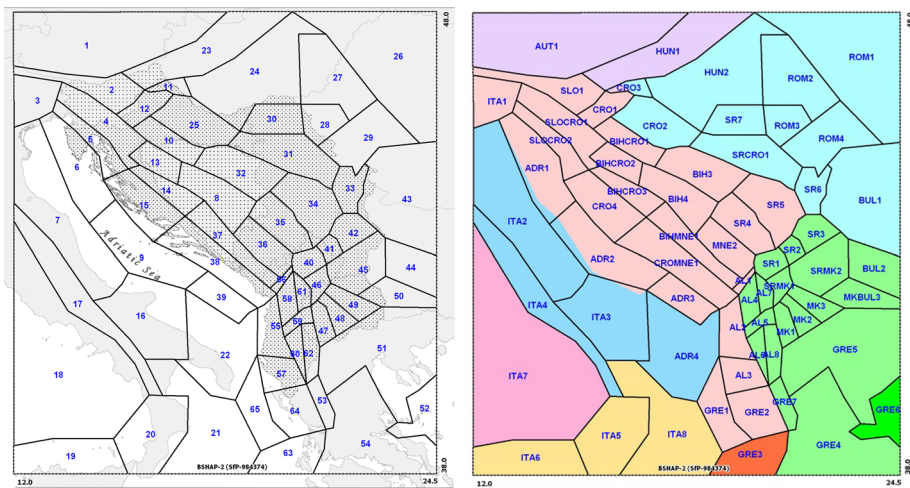


**Fig. 6** Geographical partition of SSM2’s zones and their position versus super zone model. BSHAP countries are indicated by dotted pattern

zones). Zones covering the neighboring (out-of-BSHAP) region are preserved in both models and were delineated considering SHARE project (Basili et al. 2013; Giardini et al. 2013), and according to Vamvakaris et al. (2013). Please note that the borders of the source zones are mostly consistent with the borders of the super zones since the  $b$ -value estimated for the corresponding super zone is directly implemented for the zones of SSM1 and SSM2 (Figs. 5b, 6b).

Each zone is attributed by a zone ID, covered area,  $b$ -value, maximum observed magnitude, average foci depth, and sets of weighted parameters:  $m_{\max}$ , style of faulting and fault strike angle. To assign the weights related to tectonic information, faults were grouped based on the mechanism and the median strike azimuth. Their weights were calculated based on measured length of the (grouped) faults (Poljak et al. 2000b). This “statistical” method to weight tectonic information was applied to zones in BSHAP participating countries. For zones covering non-BSHAP countries, all zones in Slovenia, zones neighboring Croatia and zones in Bosnia and Herzegovina—the weighted types and the orientation of faults were characterize using expert opinions, based on all of the above mentioned data and available literature.

In SSM1 and SSM2, the  $m_{\max}$  for each source zone was chosen by considering the largest observed magnitude in the zone. Taking into account the uncertainties related to this parameter—associated to the short time span of the BSHAP catalogue compared with the long recurrence interval of the big earthquakes, as well as the large uncertainties in the earthquake documentation and magnitude determination (especially) of the early historical events—two alternative estimates of  $m_{\max}$  are included by adding 0.25 and 0.5 magnitude units to the largest observed magnitude in each zone. In the particular geological settings—regions with low and moderate seismicity, the sparse data did not allow the determination of a reliable value of  $m_{\max}$  based on the largest observed magnitude. Therefore, we assumed that the minimum  $m_{\max}$  value in any zone cannot be lower than  $M_w = 6.0$  even if largest observed magnitude is much smaller. This assumption is consistent with the design current practice used in the BSHAP project region.

### 4.3 Smoothed activity rates and sensitivity analysis for smoothing parameters

Conditioned by the lacking of sufficient data to define a fault-based model for BSHAP region, we decided to use the seismicity-based background models in the hazard calculations. The overall method for modeling background seismicity is based on the spatial smoothing approach (Frankel 1995; Lapajne et al. 2003), whereby the rate of past earthquakes and a regionally consistent MFD are used to forecast the rate of future earthquakes. The method accounts for the spatial variability of seismicity rate, and is used for areas where faults are not known or cannot be parameterized. A grid with the dimensions of 10 km by 10 km is superimposed on the region (12.0–24.5E, 38.0–48.0N). In methodology applied—the areal seismic sources are modelled as set of the grid points included within the relevant SSMs’ polygons (zones). Earthquakes with  $M_w \geq 4.0$  that passed the completeness test of BSHAP catalogue are counted in each grid cell. Then, the annual rate of earthquakes occurrence is adjusted to account for the magnitude completeness levels. Finally, a two-stage spatial smoothing method is used to smooth the annual rates of earthquake occurrence ( $\lambda$ -grid) in each grid cell. At first, the two-dimensional isotropic Gaussian smoothing (Frankel 1995), hereinafter circular smoothing (CS), is applied to smooth the  $\lambda$ -grid. In the second stage, the fault-oriented smoothing (Lapajne et al. 2003), hereinafter elliptic smoothing (ES) that employs the seismotectonic knowledge in the

relevant source zones of SSM1 and SSM2 (main directions and types of the tectonic structures, as well as  $m_{\max}$ ) is used to model smoothed seismicity rates.

The most important factor that affects the obtained pattern of earthquake rate is the smoothing radius  $r$  ( $r$  equals  $3c$ , where  $c$  is the correlation distance and accounts for uncertainty in location of earthquakes). Sensitivity of the smoothed activity rate to the choice of smoothing radius is analyzed in Fig. 7 by using correlation distances of 15 and 45 km (comparisons for  $c = 7, 10, 15, 20, 30$  and 45 km are given in Electronic supplement). The  $c = 7$  or 10 km presented grainy patterned maps, and  $c = 30$  or 45 km spread out and smooth the seismicity too much, showing how the seismicity rate can be affected by this choice of the correlation distance. We found that the correlation distance of 10 and 15 km (assuming the error in the epicenter locations to be around 30–45 km) well-reflects the location error of historical earthquakes in the BSHAP project region. We decided to use a 10-km correlation distance i.e. a smoothing radius of 30 km along the circular smoothing.

In the case of elliptic smoothing, the extent (dimension) of smoothing is determined by the length of the rupture axis, which is computed based on the maximum magnitude. This dimension is obviously affected by zone dependent estimate of  $m_{\max}$ . For once accepted  $m_{\max}$ , the extent of smoothing will also depend on the employed empirical relationship between rupture length and  $m_{\max}$ .

Larger estimate of  $m_{\max}$  implies longer axis of elliptical smoothing, and the obtained seismicity rate is spread over larger major axes. To examine the influence of  $m_{\max}$  estimation on the obtained smoothed seismicity rate, we increased  $m_{\max}$  in each of the model's zones by 0.5 magnitude units (other parameters related to the geometry and tectonics were not changed). The absolute difference in smoothed seismicity rates for the values of  $m_{\max} + 0.5$  and  $m_{\max}$  is mostly not significant as shown in the Fig. 8c. However, extending of smoothing dimensions (e.g. in the case of  $m_{\max} + 0.5$ ) may locally reduce peaks of seismicity rate.

Additionally, we tested the compliance of the BSHAP catalogue moderate-to-large magnitude earthquake events to some of existing empirical rupture length-magnitude relations. Statistically robust global relationship of Wells and Coppersmith (1994, WC-94) considered surface rupture length (RL) and subsurface rupture length (SbRL) regressions developed for particular and for all slip-type faults events. To characterize regional rupture length and the magnitude scaling, we also utilized the relations Papazachos and

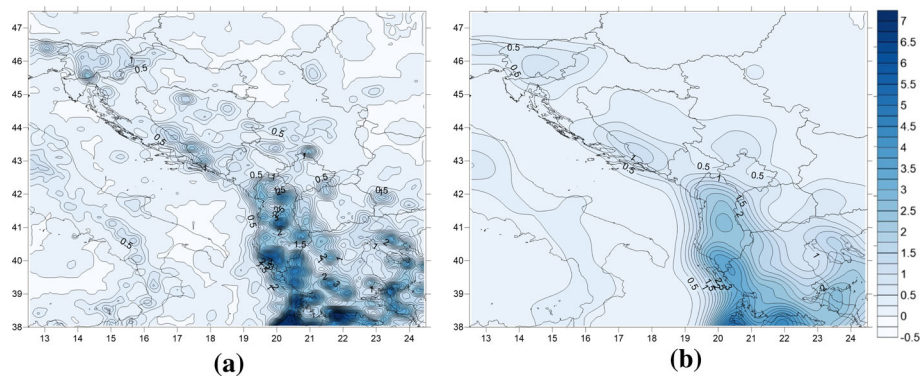


**Fig. 7** Comparison of the smoothed annual rate of earthquakes with  $M_w \geq 4.0$  in a  $10 \times 10$  km grid cell, using a correlation distance: **a**  $c = 15$  and **b**  $c = 45$  km

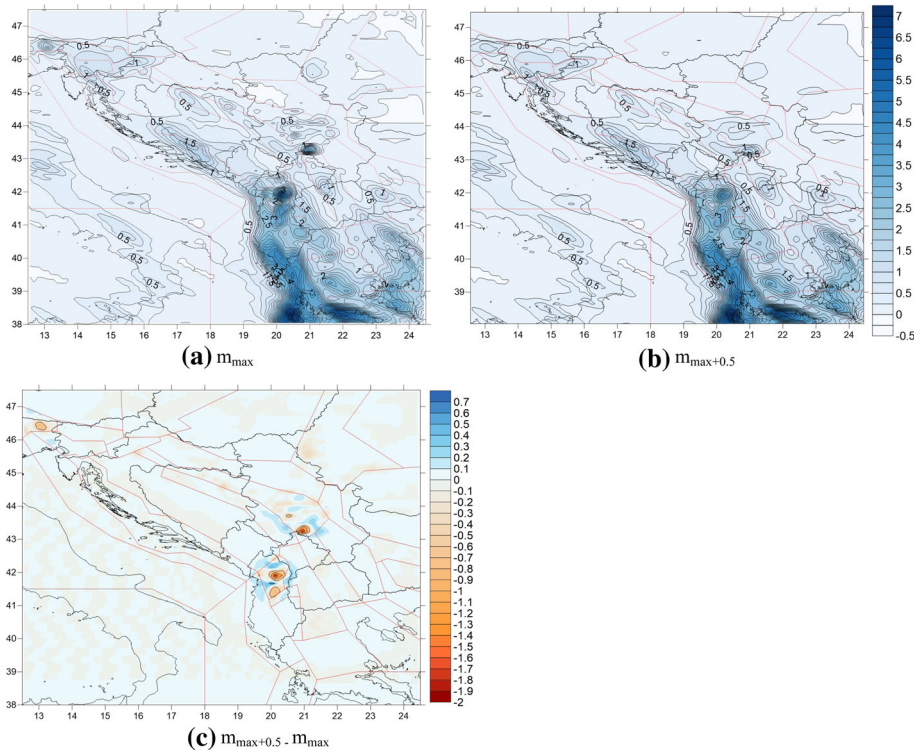


**Fig. 8** Influence of  $M_{\max}$  on elliptically smoothed annual rate of earthquakes with with  $M_w \geq 4.0$  in a  $10 \times 10$  km grid cell

Papazachou 1997 (PP-97) and Konstantinou et al. (2005, KO-05) (Fig. 10), developed on all type faults earthquake data gathered in Mediterranean region. Although opposite opinions may be found (Vakov 1996), all cited authors found that fault-type dependent regressions do not significantly influence estimated fault dimensions. Regional studies (KO-05, as well as noted by Papadopoulos et al. 2003 for the smaller magnitude events) indicate difference between regional and global relationships claiming it may be influenced by regionally variable source dimensions.

Having in mind that the aftershocks which occurred within a few hours to a few days of the main shock generally define the maximum extent of the co-seismic rupture plane (Kanamori and Anderson 1975; Dietz and Ellsworth 1990), instrumentally well recorded and documented cluster events from the BSHAP catalogue were collected and listed in Table 3. Two examples, early aftershock clusters of the 1996 Ston and 1979 Montenegro earthquakes that were used to estimate the subsurface rupture length, are shown in Fig. 9a, b).

According to Table 3, for the same  $M_w$ , the subsurface rupture lengths estimated from the Wells and Coppersmith (1994, WC-94) relation are systematically smaller than the subsurface lengths estimated from the distribution of early aftershock events in the BSHAP catalogue.

Figure 10 indicates that the data of moderate-to-large magnitude events in the BSHAP project region comply better with the regional empirical  $M_w$ - $S_b$ RL relationships (KO-05



**Table 3** Comparison of subsurface rupture lengths estimated from early shock locations in the BSHAP catalogue with ones calculated for the same Mw using the Wells and Coppersmith (1994) relations

Event time	Event ID in BSHAP Catalog	Earthquake name and location	Fault plane solution (FPS)	Mw (BSHAP catalog)	Estimated SbRL (km)	SbRL using WC-94 model for noted FPS (km)	SbRL using all slip type WC-94 model (km)
1976/05/06	9715	Friuli/Italy	TF	6.5	53	22	25
1979/04/15	10,937	Ulcinj/Montenegro coast	TF	6.9	73	38	43
1980/05/18	11,861	Kopaonik/Serbia	SS	5.9	28	12	11
1982/11/16	14,322	Fier/Albania	TF	5.6	21	7	7
1994/09/01	21,789	Bitola/Macedonia	SS	5.8	28	11	10
1995/05/13	22,402	Kozani-Grevena/Greece	NF	6.5	42	23	25
1996/09/05	25,030	Ston/Croatia	RF	6.0	38	11	13
2010/11/03	55,929	Kraljevo/Serbia	SS	5.5	27	7	6

Indicated fault type is denoted by: *TF* (thrust), *NF* (normal) and *SS* (strike slip) fault type

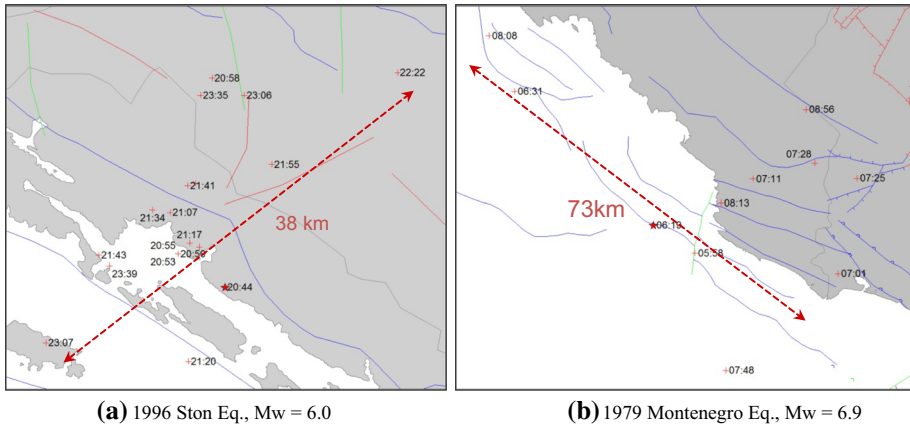


**Fig. 9** Early cluster distribution as the indicator of activated rupture length for 1996 Ston and 1979 Montenegro earthquakes based on the BSHAP earthquake catalogue. The *red star* shows the location of the mainshock and the numbers on figures indicate the times of the aftershocks

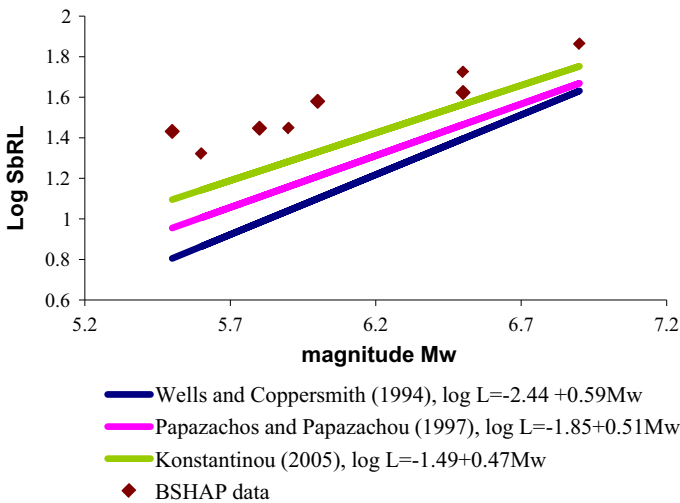


**Fig. 10** Comparison of evaluated sub surface rupture lengths of BSHAP catalogue events with estimates derived from SbRL-Mw global (WC-94 all slip-type regression) and regional models (PP-97) and (KO-05). *Smaller symbols* for the SbRL estimated from the BSHAP data imply less reliable aftershock locations

and PP-97). Having in mind that estimated source geometry is strongly affected by accuracy of event’s location, in the Fig. 10—by smaller symbols, we indicated all events dated before year 1983 (as the step-stone in regional seismic network development).

Although the differences between the BSHAP data and the regional model predictions are also evident (even for the post-1983 events), the compliance of presented data to global one is even more pronounced. Since the BSHAP dataset itself is statistically insufficient to derive any reliable magnitude scaling relation, we concluded to use Konstantinou et al. (2005) sub surface rupture length-magnitude relation in the present study.

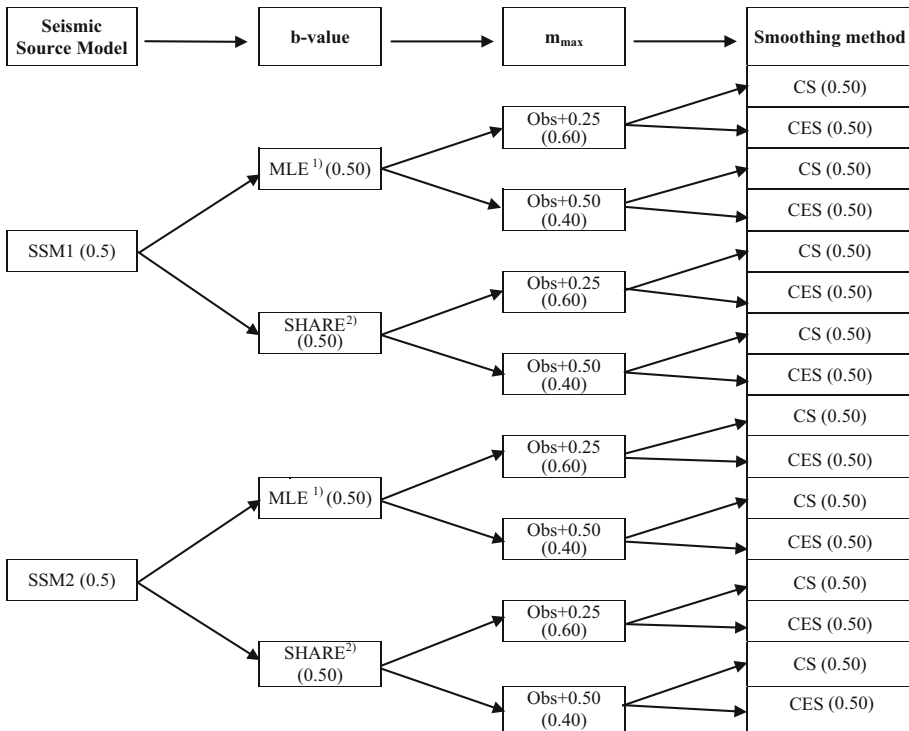


**Fig. 11** Logic tree for the background-gridded seismic source model for BSHAP project area b-value estimation: (1) Average value of Weichert and KS-92 MLE, (2) AS denotes Areal Source model of SHARE

**4.4 BSHAP logic tree for the seismic source characterization**

The ground motion characterization logic tree used in the PSHA calculations for the hazard maps of the Western Balkan region was provided in Šalic et al. (2016). Details of the logic tree for the seismic source characterization models that incorporates the epistemic uncertainties associated with construction of the seismic source models and some chosen parameters are provided in Fig. 11. Each node in the logic-tree defines the alternative model or ‘branch’ in the logic-tree, with weights that sum to one. The first node in the logic tree shows two source zonation models that are considered: SSM1 and SSM2. The weights accepted for these models are 0.50 and 0.50 respectively.

The second node accounts for uncertainty in the b-value estimation. Two alternative estimates for the b-value are used for each source zone: (1) the average value of the relevant estimates derived using the super zones sub-catalogs, considering the variable magnitude completeness MLE (Weichert 1980), and the estimates obtained using the Kijko and Sellevoll (1992) approach on the same sub-catalogs; (2)  $b = 1.0$  for all the source zones, as comparable to the AS model of the SHARE project (Giardini et al. 2013).

Third node in the Fig. 11 represents the epistemic uncertainty on the maximum magnitude ( $m_{max}$ ). Two alternative estimates of  $m_{max}$  are assigned to every source zone. These are obtained by adding 0.25 and 0.5 magnitude units, respectively, to the largest observed magnitude in the relevant seismic source model, or the value  $M_W$  6.0 is accepted as the

floor for  $m_{\max}$  in the regions with low and moderate seismicity. This two-level logic tree branch was associated with the weights of 0.6 and 0.4 respectively.

The last node in the Fig. 11 shows the uncertainty related to the spatial smoothing approach. To account for the influence of the smoothing method on the seismic hazard, two alternative smoothing algorithms are employed. Based on the sensitivity analysis provided in the previous section, we decided to use: (1) the circular spatial smoothing (CS) with a smoothing radius  $r = 30$  km and (2) both the circular (with  $r = 30$  km), and elliptic smoothing (CES) which also considers the rupture directions in the seismic source zones based on the seismotectonic data. Thus, the spatial smoothing is considered as a branch level in the logic-tree structure describing the epistemic uncertainties associated with the type of smoothing. We assign the same weight (0.5) to both CS and CES smoothing algorithms.

## 5 Conclusions

This article presents the seismic source characterization model developed within the course of the BSHAP project and the associated logic tree that will be implemented in the PSHA calculations for the harmonized seismic hazard maps of the Western Balkan region. Developed model represents the expert opinion available in the region, specifically the experts from the Institute of Geosciences, Energy, Water and Environment (Tirana, Albania), Faculty of Science, University of Zagreb (Croatia), Institute of Earthquake Engineering and Engineering Seismology (Skopje, Macedonia), Institute of Hydrometeorology and Seismology of Montenegro, Seismological Survey of Serbia, and the Environmental Agency of the Republic of Slovenia.

The seismic source models developed for BSHAP project covers the territory of BSHAP partner countries and countries surrounding the BSHAP area. Since the information related to the active faults, fault segmentation models, rupture process documentation, and seismic moment accumulation for the broader BSHAP region is not homogeneous, planar fault based source characterization models could not be developed in the course of this project. Instead, the PSHA approach that depends on the earthquake catalogue, magnitude recurrence model, and smoothed seismicity rates is applied. The key fundamental input of the process is the uniform and updated BSHAP earthquake catalogue, which was unified from the national catalogues of data providers in the BSHAP area. The BSHAP catalogue is supported by the FPS database developed by the BSHAP participants in developing the SSC models. At first, a super zone model (SZM) is created and used for estimating the stable  $b$ -values. The delineation of the super zones was based on the alternative zonation models (SSM1 and SSM2) with merging seismic source zones, considering the FPS database, relevant tectonic information, dominating stress regime, and the zone-specific catalogue completeness levels. In addition, two alternative models SSM1 and SSM2 are developed for the two-stage spatial smoothing of the seismicity rates. All available information regarding the geodynamics of the region and fault activity is combined with the regional expertise in source zonation to depict local tectonic features. Adopted maximum magnitudes in zones of SSMs are locally influencing extension of smoothing but the hazard estimates as well, and are dependent to observed magnitudes.

The SSC models developed during the course of BSHAP are documented in this manuscript to serve as a valuable source for the relevant ongoing research of local

scientists. All details on adopted seismic sources are provided in the Electronic Supplement of this manuscript.

**Acknowledgements** This work is funded by NATO SfP Program under: “Improvements in the Harmonized Seismic Hazard Maps for the Western Balkan Countries” project” (NATO SfP Award Number: 984374). BSHAP participants are indebted to the institutions/data providers for positive cooperative attitude in data releasing and continuous support. We, the BSHAP projects teams and authors of this paper, do expect that NATO, Public Diplomacy Divisions’ expectations and policies are met, in terms of technical and synergic achievements, and that BSHAP’s results justify granting that we highly acknowledge. We would like to extend our sincere gratitude to Prof. M. Herak who kindly provided his FPS calculation software. The MathLab computer code used for Kijko and Sellevoll (1992) tests was the courtesy of Prof. Kijko, provided for research purposes only.

## References

- Aliaj SH (1998) Neotectonic structure of Albania. *J Nat Tech Sci* 4:15–42
- Bada G, Horváth F, Dövényi P, Szafián P, Windhoffer G, Cloetingh S (2007) Present-day stress field and tectonic inversion in the Pannonian basin. *Glob Planet Change* 58:165–180
- Basili R, Kastelic V, Demircioglu MB, García Moreno D, Nemser ES, Petricca P, Sboras SP, Besana-Ostman GM, Cabral J, Camelbeek T, Caputo R, Danciu L, Domac H, Fonseca J, García-Mayordomo J, Giardini D, Glavatovic B, Gulen L, Ince Y, Pavlides S, Sesetyan K, Tarabusi G, Tiberti MM, Utkucu M, Valensise G, Vanneste K, Vilanova S, Wössner J (2013) The European database of seismogenic faults (EDSF) compiled in the framework of the project SHARE. <http://diss.rm.ingv.it/share-edsf/>, doi: [10.6092/INGV.IT-SHARE-EDSF](https://doi.org/10.6092/INGV.IT-SHARE-EDSF)
- Blašković I (1998) The two stages of structural formation of the coastal belt of the external dinarides. *Geol Croat* 51:75–89
- Brückl E, Behm M, Decker K, Grad M, Guterch A, Keller GR, Thybo H (2010) Crustal structure and active tectonics in the Eastern Alps. *Tectonics*. doi:[10.1029/2009TC002491](https://doi.org/10.1029/2009TC002491)
- Burchfiel BC, King RW, Todosov A, Kotzev V, Dumurdzanov N, Serafimovski T, Nurce B (2006) GPS results for Macedonia and its importance for the tectonics of southern Balkan extensional system. *Tectonophysics*. doi:[10.1016/j.tecto.2005.10.046](https://doi.org/10.1016/j.tecto.2005.10.046)
- Čejkovec V, Pekevski L, Černih D (2008) Source mechanism of the 1994 September 1 M-L = 5.2 Bitola earthquake. *Contrib Sec Math Tech Sci XXIX(1–2)*:37–48
- Cloetingh SÁPL, Horvath F, Bada G, Lankreijer AC (2002) (eds). Introduction: Neotectonics and surface processes: the Pannonian Basin and Alpine/Carpathian System. EGU Stephan Mueller Special Publication Series, 3, 1–7, 2002, European Geosciences Union
- Cushing EM (1985) Evolution structurale de la marge Nord-Ouest hellénique dans l’île de Levkas et ses environs (Grèce nord-occidentale). These de troisième cycle Univ, Paris XI - Orsay, p 297
- Dietz LD, Ellsworth WL (1990) The October 17, 1989, Loma Prieta, California, earthquake and its aftershocks: geometry of the sequence from high-resolution locations. *Geophys Res Lett* 17:1417–1420
- Dumurdzanov N, Serafimovski T, Burchfiel BC (2005) Cenozoic tectonics of Macedonia and its relation to the South Balkan extensional regime. *Geosphere* 1(1):1–22. doi:[10.1130/GES00006.1](https://doi.org/10.1130/GES00006.1)
- Frankel AD (1995) Mapping seismic hazard in the Central and Eastern United States. *Seismol Res Lett* 66(4):8–21
- Frashëri A, Bushati S, Bare V (2009) Geophysical outlook on structure of the Albanides. *J Balkan Geophys Soc* 12(1):9–30
- Giardini D, Woessner J, Danciu L, Crowley H, Cotton F, Grünthal G, Pinho R, Valensise G, Akkar S, Arvidsson R, Basili R, Camelbeek T, Campos-Costa A, Douglas J, Demircioglu MB, Erdik M, Fonseca J, Glavatovic B, Lindholm C, Makropoulos K, Meletti C, Musson R, Pitilakis K, Sesetyan K, Stromeyer D, Stucchi M, Rovida A (2013) Seismic hazard harmonization in Europe (SHARE): online data. Resource. doi:[10.12686/SED-00000001-SHARE](https://doi.org/10.12686/SED-00000001-SHARE)
- Heidbach O, Tingay M, Barth A, Reinecker J, Kurfeß D, Müller B (2008) The world stress map database release 2008. doi:[10.1594/GFZ.WSM.Rel2008](https://doi.org/10.1594/GFZ.WSM.Rel2008)
- Herak M, Herak D, Markušić S (1995) Fault-plane solutions for earthquakes (1956–1995) in Croatia and neighbouring regions. *Geofizika* 12:43–56

- Herak M, Herak D, Dasović I (2016) Fault-plane solutions and stress orientation in the greater region of Northern and Central Dinarides. In: 35th general assembly of the European Seismological Commission. Trieste, Italy, 4–11 Sept 2016
- Jouanne F, Mugnier JL, Koçi R, Bushati S, Matev K, Kuka N, Shinko I, Koçiaj S, Duni L (2012) GPS constrains on current tectonics of Albania. *Tectonophysics* 554:50–62
- Kaluderovic N (2015) Focal mechanisms and tectonic stress in Montenegro. In: 4th NATO Project No 984374 Meeting. Podgorica, Montenegro, 26–27 March 2015
- Kanamori H, Anderson DL (1975) Theoretical basis for some empirical relations in Seismology. *Bull Seismol Soc Am* 65:1073–1095
- Kastelic V, Carafa MMC (2012) Fault slip rates for the active External Dinarides thrust-and-fold belt. *Tectonics*. doi:[10.1029/2011TC003022](https://doi.org/10.1029/2011TC003022)
- Kijko A, Sellevoll MA (1992) Estimation of earthquake hazard parameters from incomplete data files. Part II: incorporation of magnitude heterogeneity. *Bull Seismol Soc Am* 82(1):120–134
- Koçi R (2014) Geodynamics and cinematics of nowadays movements in Albania., *J Nafta Shqiptare* 1:40–45
- Koçi R, Duni LI, Begu E, Bozo RR (2013) Geodynamic characteristics of Albanian territory. In: 7-th congress of Balkan Geophysical Society. Tirana, Albania, 7–10 Oct 2013
- Konstantinou KI, Papadopoulos GA, Fokaefs A, Orphanogiannaki K (2005) Empirical relationship between aftershock area dimensions and magnitude for earthquakes in the Mediterranean Sea region. *Tectonophysics* 403:95–115
- Lapajne JK, Šket Motnikar B, Zupančič P (2003) Probabilistic seismic hazard assessment methodology for distributed seismicity. *Bull Seismol Soc Am* 93(6):2502–2515
- Markušić S, Gülerce Z, Kuka N, Duni L, Ivančić I, Radovanović S, Glavatović B, Milutinović Z, Akkar S, Kovačević J, Mihaljević J, Šalić R (2016) An updated and unified earthquake catalogue for the Western Balkan Region. *Bull Earthq Eng* 14(2):321–343. doi:[10.1007/s10518-015-9833-z](https://doi.org/10.1007/s10518-015-9833-z)
- McKenzie D (1972) Active tectonics of the mediterranean region. *Geophys J R Astron Soc* 30:109–185. doi:[10.1111/j.1365-246X.1972.tb02351.x](https://doi.org/10.1111/j.1365-246X.1972.tb02351.x)
- Mercier JL, Delibassis N, Gauthier A, Jarrige JJ, Lemeille F, Philip H, Sebrier M, Sorel D (1979) La néotectonique de l'arc égéen. *Rev Géog Phys Géol Dyn XXI(1):67–92*
- Mladenović A, Trivić B, Antić M, Cvetković V, Pavlović R, Radovanović S, Fügenschuh B (2014) The recent fault kinematics in the westernmost part of the Getic nappe system (Eastern Serbia): evidence from fault slip and focal mechanism data. *Geol Carp* 65(2):147–161
- Papadopoulos GA, Karastathis VK, Ganas A, Pavlides S, Fokaefs A, Orfanogiannaki K (2003) The Lefkada, Ionian Sea (Greece), shock (Mw 6.2) of 14 August 2003: evidence for the characteristic earthquake from seismicity and ground failures. *Earth Planets Space* 55:713–718
- Papazachos BC, Papazachou C (1997) The Earthquakes of Greece. Ziti Editions, Thessaloniki
- Poljak M, Živčić M, Zupančič P (2000a) The seismotectonic characteristics of Slovenia. *Pure appl Geophys* 157:37–55
- Poljak M, Zupančič P, Lapajne JK, Šket Motnikar B (2000) Seismotectonic input for spatially smoothed seismicity approach. In: Proceedings of seismicity modeling in seismic hazard mapping workshop, Poljče, Slovenia
- Pondrelli S, Salimbeni S, Ekström G, Morelli A, Gasperini P, Vannucci G (2006) The Italian CMT dataset from 1977 to the present. *Earth Planet Int Phys* 159(3–4):286–303. doi:[10.1016/j.pepi.2006.07.008](https://doi.org/10.1016/j.pepi.2006.07.008)
- Šalić R, Sandikkaya MA, Milutinović Z, Gülerce Z, Duni L, Kovačević V, Markušić S, Mihaljević J, Kuka N, Kaludjerović N, Kotur N, Krmptić S, Kuk K, Stanko D (2016) BSHAP project strong ground motion database and selection of suitable ground motion models for the Western Balkan Region. *Bull Earthq Eng*. doi:[10.1007/s10518-016-9950-3](https://doi.org/10.1007/s10518-016-9950-3)
- Scordilis EM, Karakaisis GF, Karacostas BG, Panagiotopoulos DG, Comninakis PE, Papazachos BC (1985) Evidence for transform faulting in the Ionian Sea: the Cephalonia Island earthquake sequence of 1983. *Pure appl Geophys* 123:388
- Sorel D (1976) Etude neotectonique dans l' Arc Egeen occidentale: les iles Ioniennes de Kephallinia et Zakynthos et l'Elide occidentale. These 3e cycle. Universite de Paris-Sud, Orsay
- Sorel D (1989) L'evolution structural de la Grece Nord-occidentale depuis le Miocene dans le cadre geodynamique de l'Arc Egeen These d' Etat. Universite de Paris-Sud, Orsay
- Šumanovac F, Orešković J, Grad M, ALP 2002 Working Group (2009) Crustal structure at the contact of the Dinarides and Pannonian basin based on 2-D seismic and gravity interpretation of the Alp07 profile in the ALP2002 experiment. *Geophys J Int* 179:615–633. doi:[10.1111/j.1365-246X.2009.04288.x](https://doi.org/10.1111/j.1365-246X.2009.04288.x)
- Tari-Kovačić V, Mrinjek E (1994) The role of palaeogene clastics in the tectonic interpretation of Northern Dalmatia (Southern Croatia). *Geol Croat* 47:127–138

- Tomljenović B, Csontos L, Márton E, Márton P (2008) Tectonic evolution of the northwestern internal dinarides as constrained by structures and rotation of Medvednica Mountains, North Croatia. *Geol Soc Lond Spec Publ* 298:145–167. doi:[10.1144/SP298.8](https://doi.org/10.1144/SP298.8)
- Vakov AV (1996) Relationship between earthquake magnitude, source geometry and slip mechanism. *Tectonophysics* 261:97–113
- Vamvakaris DA, Papazachos CB, Papaioannou C, Scordilis EM, Karakaisis GF (2013) A detailed seismic zonation model for shallow earthquakes in the broader Aegean area. *Nat Hazards Earth Syst Sci Discuss* 1:6719–6784. doi:[10.5194/nhessd-1-6719-2013](https://doi.org/10.5194/nhessd-1-6719-2013)
- Vannucci G, Gasperini P (2003) A database of revised fault plane solutions for Italy and surrounding regions. *Comput Geosci* 29:903–909
- Weichert D (1980) Estimation of the earthquake recurrence parameters for unequal observation periods for different magnitudes. *Bull Seismol Soc Am* 70:1337–1346
- Wells DL, Coppersmith KL (1994) New empirical relationship among magnitude, rupture length, rupture width, rupture area, and surface displacement. *Bull Seismol Soc Am* 84(4):974–1002
- Wiemer S, Wyss M (2000) Minimum magnitude of completeness in earthquake catalogs: examples from Alaska, the Western United States, and Japan. *Bull Seismol Soc Am* 90(4):859–869
- Woessner J, Danciu L, Giardini D, Crowley H, Cotton F, Grünthal G, Valensise G, Arvidsson R, Basili R, Demircioglu MN, Hiemer S, Meletti C, Musson RW, Rovida AN, Sesetyan K, Stucchi M, the SHARE consortium (2015) The 2013 European seismic hazard model: key components and results. *Bull Earthq Eng*. doi:[10.1007/s10518-015-9795-1](https://doi.org/10.1007/s10518-015-9795-1)